MIRAS IMU prestudy

Eileen Kränzle

06.08.2022 - 15.10.2022

Contents

1 Introduction

The mitochondrial recessive ataxia syndrome (MIRAS) is a heritable neurodegenerative disease, first reported about in the early 2000s. With a relatively high carrier frequency of 1:125 it is one of the most common ataxias in Finland, however, it can also be found in other northern European countries [1]. It is caused by a mutation in the POLG gene affecting the function of the γ-polymerase, the only DNA polymerase in human mitochondria [2]. Symptoms as well as the age of onset vary greatly between patients which makes standardized treatment difficult. Under common symptoms fall epilepsy, ataxia, peripheral neuropathy, involuntary movements, and cognitive impairment [1]. Very little is known about the neurological and muscular underlying processes of MIRAS and up to know, MIRAS cannot be cured. The treatment is only symptomatic [3] and consists of subjective ratings of the therapists, for example, by using ataxia rating scales such as the scale for the assessment and rating of ataxia (SARA) [4]. However, those regular visits at the clinic are time-consuming and therefore associated with great effort for the therapist as well as the patient since many patients live far in the countryside of Finland.

This effort could be reduced by home-based assessments of the disease using wearable sensors. For other neurological diseases such as Parkinson or Friedreich's ataxia home-based assessments have shown a strong correlation to clinical assessments [5,6]. Further, the SARA scale has successfully been implemented as a video-based instrument allowing assessing ataxia tests at home [7]. Remote monitoring for MIRAS would save time as well as gives the opportunity to perform clinical tests on a more frequent basis. This might also give the doctors better insights into the progression of the disease.

In a previous study the muscle activity of MIRAS patients and control subjects for different ataxia assessment tasks were measured using EMG sensors [8]. An analysis of the EMG data showed characteristics indicating MIRAS ataxia, but revealed some limitations of the method too. Since the study also measured IMU signals with a sensor but didn't perform an in-depth analysis of the IMU data, we want to examine the previously measured IMU data to explore another method of monitoring the disease.

In recent years, different ataxia diseases have been investigated with IMU sensors [9–15]. These studies showed the success in using IMU sensor for detecting ataxia from gait [9, 10] and various ataxia tests such as the Romberg's test, [10, 11] or upper limb tests like the Finger-to-nose test [12–15]. Some studies have further successfully applied machine learning techniques to distinguish ataxia patients from healthy controls using IMU sensors [12, 13]. This shows the potential IMU sensors bring to track the progression of MIRAS. IMU sensors also can bring the advantage of measuring movements that may be difficult to detect with the naked eye.

The development of a remote monitoring application for MIRAS using IMU would be promising in the future. Therefore, this study investigates the previously measured IMU data [8] in more detail. Our goal is to identify promising tasks showing differences in the MIRAS patient and control subjects to determine a task set that could be used for home-based IMU assessment. Additionally, we want to obtain the most meaningful features that could be used for rating the progression of MIRAS.

2 IMU Data Analysis 2021

This section describes the analysis and results of the IMU data collected in 2021 during the sEMG measurements.

2.1 Material and Methods

The data used for this analysis is data that was collected in 2021 for the EMG analysis.

2.1.1 Data collection

The measurements were done with the Delsys Trigno Quattro EMG Sensors that include a three axis IMU sensor and four EMG sensors. Because different IMU sensors have unique gyroscope offsets, I have identified the sensor with number 00285 as the sensor used for all participants to record the IMU data (see Sensor Comparison directory).

An IMU sensor is a measuring device which can be used to track movements of objects or people. It consists of an accelerometer which measures the acceleration, a gyroscope which measures the angular velocity and a magnetometer that measures the magnetic field.

In the study setting, the IMU sensor was placed on the back of the hand with the arrow on the sensor pointing in proximal direction. Therefore, the x-axis of the sensor follows the radial and ulnar axis, the y-axis follows the distal proximal axis and the z axis follows the dorsal ventral axis.

The previous study of 2021 consisted of one MIRAS patient and seven control subjects of which one was matched in terms of weight. However, IMU data was only available for five out of seven control subjects. This results in a relatively small dataset (see tab. 1). The MIRAS patient has the ID MR and there is also a weight matched control with the ID VR.

ID	Date	Gender	Handedness	Age [years]	Weight [kg]	Height [cm]
QR	23.08.2021	M	R	43	71	178
SR	10.08.2021	F	R	23	58	168
RR	17.08.2021	M	R	28	96	185
VR	20.08.2021	M	R	51	133	173
UR	23.08.2021	M	R	28	82	181
MR	20.07.2021	M	R	42	132	180

Table 1: Overview Participants study 2021

There was a task set consisting out of 21 tasks in total. In this analysis we will analyze the static tasks and the repetition tasks consisting of seven respectively six tasks each. Some tasks, such as the pointing tasks are performed multiple times by each patient. A detailed description of the tasks can be found in the documents of the EMG study from 2021.

2.1.2 Data pre-processing

The data pre-processing includes several steps to obtain a signal that can be analyzed easily and of which features can be extracted.

Because we want to extract different features depending on the task type, the data pre-processing has small differences to achieve the best pre-processing for each task.

The data contains zeros at the beginning of the measurement, which occur because of a Bluetooth connection problem. Therefore, those zeros are removed for all tasks. Additionally, for two subjects, one task out of the static task set was cut at the beginning respectively the end because there were abnormally high peaks that can not be explained by the performed movement. The repetitive tasks were further cut exactly at the beginning and the end of the repetitions because this is also done for the analysis of 2022. It also has to be noted, that sometimes the data of 2021 does not capture the whole repetition because of a recording delay. In these cases the data was cut in a way that there were no half repetitions. This is why sometimes the total number of repetitions does not match the number of repetitions done in reality.

Because the accelerometer of the sensor measures the gravity which is not relevant for the movement of the patient, the gravity is removed by using a Madgwick filter [16]. The gyroscope data is further converted from degrees per second into radians per second, since the Madgwick filter requires the gyroscope data in this unit. Furthermore, the gyroscope data has a small sensor-individual offset and therefore is mean centered. The Madgwick filter computes for each time point the relative location of the sensor to the earth and outputs those rotations as quaternions. Knowing the rotation of the sensor, the direction of the gravity can be computed and subtracted from the acceleration for each data point. This step is performed for all tasks.

For the repetition tasks, a low pass filter with a cutoff frequency of 20 Hertz is added to further smoothen the signal. It is only applied to the repetitive tasks, because the movements for the repetitive signals are larger and therefore the relevant frequencies are relatively small. For the static tasks, in an ideal execution, there should be no movements visible, and therefore the signal should rather consist of high frequency components. To preserve the high frequency components, no low pass filter is applied to this data.

2.1.3 Tasks and Feature extraction

Table 2 shows the number of recorded tasks for each task and subject in the previous EMG project. Since the relaxation and maximal voluntary contraction tasks were done to normalize the EMG data to the maximal electrical activity to make the subjects comparable, for this analysis, those tasks are left out. The exhaustion tasks are left out as well because they do not add much to the analysis of the static tasks and have already been analyzed in terms of holding time in the EMG analysis. Moreover, we leave the wrist movement tasks out, because the patient had difficulties performing them. Therefore, we are left with two task sets, the repetition tasks and the static tasks, that we will analyze in the following.

Task Type	Task	MR	QR	RR	SR	UR	VR
Repetition	point standard	4	3	3	3	3	3
	point 0.5kg	1	2	2	2	2	2
	point w/ pause	1	1	1	1	1	1
	left/right standard	1	1	1	1	1	1
	left/right 0.5kg	1	1	1	1	1	1
	pro/supi normal	1	1	1	1	1	1
	pro/supi 0.5kg	0	1	1	1	1	1
Relaxation	relax hanging	1	1	1	1	1	1
	relax on lap	1	2	2	2	2	2
Maximal Voluntary Contraction	flex MVC	2	3	2	1	3	3
	ext MVC	3	3	3	2	3	3
Static	flex static 0kg	1	1	1	1	1	1
	flex static 0.5kg	1	1	1	1	1	1
	flex static 2kg	1	1	1	1	1	1
	flex static 3kg	1	1	1	1	1	1
	ext static 0kg	1	1	1	1	1	1
	ext static 0.5kg	1	1	1	1	1	1
	ext static 2kg	1	1	1	1	1	1
Exhaustion	flex exhaust 2kg	1	1	1	1	1	1
	ext exhaust 2kg	1	1	1	1	1	1
Other	wrist movements	1	1	1	1	1	0

Table 2: Overview: Number of recorded tasks for each subject

Repetition tasks

Seven out of the 21 tasks performed were tasks to perform a movement repetitively. These tasks are the pointing task and the pointing task with pauses, the task in which a cup is moved from left to right and back and the hand rotation task (pronation/supination). Some of these tasks were

also performed with a weight. However, for one task out of those, the pro/supi 0.5 kg task, there is no data available for the patient and therefore this task isn't considered in the analysis.

For the repetition tasks it is useful to not only look at the signals as a whole but also compare the different repetitions of the task. For this purpose, the signals needs to be split into single repetitive sections of the task. Because the repetitions are very prominent in the magnetometer and the gyroscope signal and the accelerometer signal does not show the repetitions very clearly only those two signals are used to determine the splitting points.

This is done by extracting the maximal autocorrelation of the signals which results in a set of candidate signal splitting points for each axis for the gyroscope and magnetometer signal making up six sets in total. Then, the splitting points of all six splitting point sets are clustered together and only splitting points that are supported by at least four splitting candidates are kept. The mean of these clusters is computed and added to the final splitting points. Furthermore, some fine-tuning is done to handle missing and wrong splitting points.

Given the splitting points, the repetition period can be extracted which is simply the time between two splitting points. Furthermore, all pairwise repetition correlations are computed for all three signals. For the accelerometer and gyroscope signal the maximal amplitude is also computed for each repetition.

As the high frequency components give a measure for irregularities, these were extracted before the signal was smoothened with the low-pass filter. A cutoff frequency of 5 Hertz was chosen because all frequencies below 5 Hertz could be involved in the signal. Then the standard deviation of the high frequency components was computed.

Static tasks

Another seven out of the 21 tasks performed were tasks involving static contractions. The static tasks can be divided into two groups, one that mainly stressed the elbow flexor muscles and one that mainly stressed the triceps as an extensor muscle. The flexor task was performed four times: without additional weight, with additional 0.5 kg weight, with additional 2 kg weight and with additional 3 kg weight. The extensor task was performed three times: without additional weight, with additional 0.5 kg weight and with additional 2 kg weight.

For these tasks, the standard deviation of the accelerometer and the gyroscope signal was computed. Further, the number of mean crossings and the peak count, both relative to the signal length, was determined. In the frequency domain, the spectral energy of 4 Hertz windows was computed. Each window overlapped by 50% with the previous and next window.

2.2 Results and Discussion

2.2.1 Repetition tasks

Repetition period

Since MIRAS goes along with movement difficulties, we expected the patient to perform the movement slower. Therefore, we computed the confidence intervals of the signal period for each task.

For some of the tasks we observe higher signal periods for the MIRAS patient than for the control subjects (see fig. 1). However, there are also tasks, that do not show this trend. One of those is for example the pointing task with pauses. Here, possibly varying pause lengths could impact the signal period and therefore the signal period might not yield meaningful information for this task. All in all, the differences between patient and control subjects are not very clear, so this feature should be investigated further.

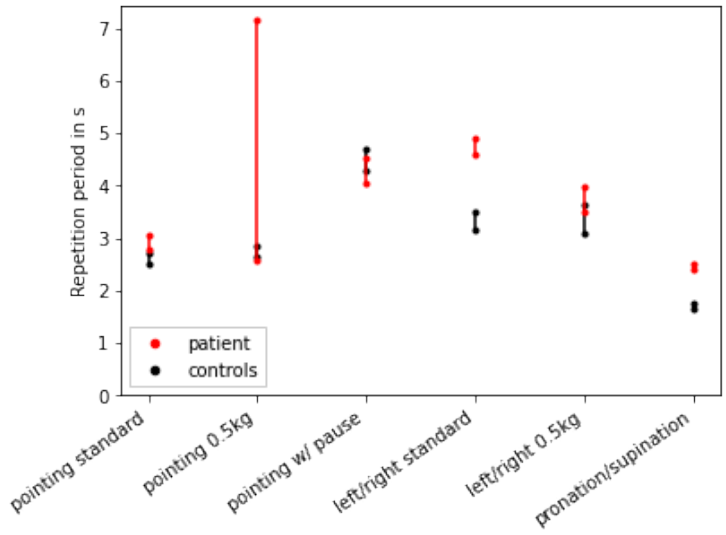

Figure 1: Confidence intervals of the repetition periods for all different repetition tasks

Repetition correlation

Since clinical manifestations of MIRAS further include involuntary movements, we analyzed the similarities between the executed repetitions of the patient by computing the repetition correlation.

Interestingly, when analyzing the computed confidence intervals of the repetition correlation, the gyroscope signal was the most meaningful. It was the only signal, that showed clear differences between patient and control in terms of correlation. We expected all signals to have a similar correlation, however, the acceleration signal seems to be very sensitive to small movements, while on the other hand the magnetometer signal seems to be very stable to small movements. Therefore, only the gyroscope signal is considered for the correlation analysis.

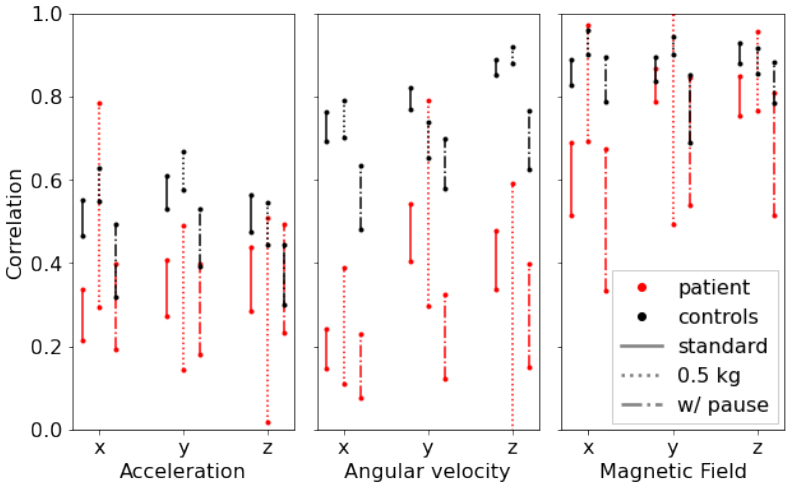

Figure 2: Confidence intervals of the pairwise correlation between all repetitions for the pointing tasks for all three axes (x, y, z) and signals (accelerometer, gyroscope, magnetometer)

As expected, fig. 2 shows that the patient has overall a significantly lower correlation of repetitive tasks. This indicates that the MIRAS patient cannot perform the tasks as regular as the control subjects possibly due to involuntary movements caused by the ataxia. Further, the correlation of the pointing task with pauses is generally lower than the pointing task. Similar to the repetition period this might occur because of varying pause times. Because of the highly

significant differences between patient and control overall, we consider the repetition correlation as a key feature for detecting MIRAS with an IMU sensor.

The results of the other repetition tasks are not as meaningful as the pointing tasks. Similar results can be observed for the left/right task, however, the differences between patient and control are not as pronounced as for the pointing task here. This could be due to the smaller amount of data for this task. Therefore, with a larger amount of data tasks involving big movements such as the left/right task could possibly distinguish the patient from the control subjects by repetition correlation as well. The pronation and supination task on the other hand only shows a difference between patient and control for the magnetometer signal. Against our expectations the patient showed a higher correlation than the control subjects for this signal. A possible reason for this unexpected result could be the short signal period of the control subjects for this task which makes a regular movement more difficult than performing the task at slower speed as the patient did. Further, the task involved smaller movements which might be more difficult to perform as similar as greater movements.

Repetition amplitude

Another measure to investigate involuntary movements caused by MIRAS might be the maximal amplitude of each repetition.

Fig. 3 shows that the MIRAS patient has in general a much higher maximal amplitude than the controls subject for the pointing tasks. A higher amplitude of both acceleration and angular velocity indicates a more sudden movement, whereas a lower amplitude indicates a smoother movement. This is especially pronounced in the unweighted tasks. The task with a 0.5 kg weight has overall a lower amplitude which can be explained by the weight slowing down the movements in general and accordingly the amplitude as well. Therefore, for further studies a weighted task may not suitable because it influences the task execution in a non-natural way.

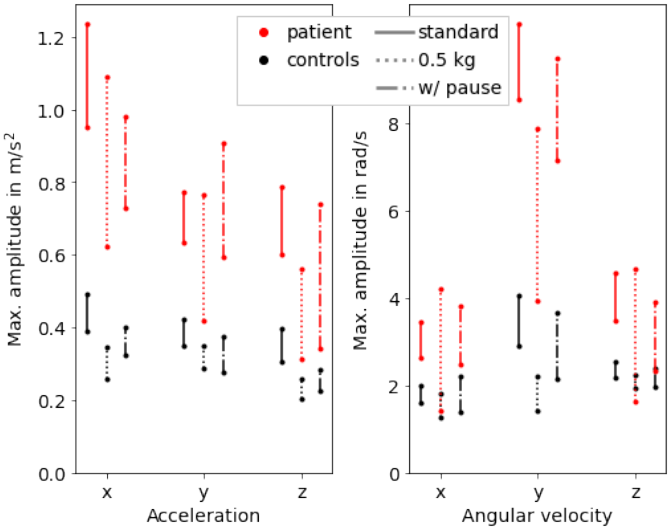

Figure 3: Confidence intervals of the maximal amplitudes of all repetitions for the left/right tasks for all three axes (x, y, z) and signals (accelerometer, gyroscope)

In addition to that, the single axes yield information about the direction of the task execution. Especially the x-axis for the acceleration data stands out, which is for most subjects the main axis along which the task is executed. The same goes for the y-axis of the gyroscope data, which is for most subjects the main rotation axis. Therefore, we can conclude that the expected movement from nose to the edge of the monitor is more sudden. However, because the other two axes also show a significantly higher amplitude, there are also more sudden movements that do not seem to be related to the task, which indicates a higher number of involuntary movements overall.

The analysis of the other repetitive tasks is less meaningful. A higher amplitude for the patient can only be observed in the weighted left/right task for the acceleration signal. The gyroscope

signal and the unweighted left/right task do not show this trend. Nevertheless, this might again be due to the small amount of data available. The pronation and supination task also does not show any trends as well.

Frequency Domain

Besides the amplitude and the correlation of the signal, a measure for evaluating the smoothness of the signal is useful.

Fig. 4 shows that the patient has the highest amount of high frequency components for all axes of both, the accelerometer signal and the gyroscope signal.

This indicates that the control subjects perform the task smoother than the patient. A closer look at the axes shows that again the standard deviation along the main acceleration axis x and the main rotation axis y are the most dominant. This indicates that mainly the movement itself was lacking smoothness. Nevertheless, the matched control shows also a higher amount of high frequencies. So the high frequency components could also occur because of a higher age or weight and not solely because of the ataxia.

The other tasks showed similar results, but the features weren't as pronounced as in the pointing task. Reasons for that could be again the small amount of data available for this task for the left/right task or a faster task execution for the pronation and supination task.

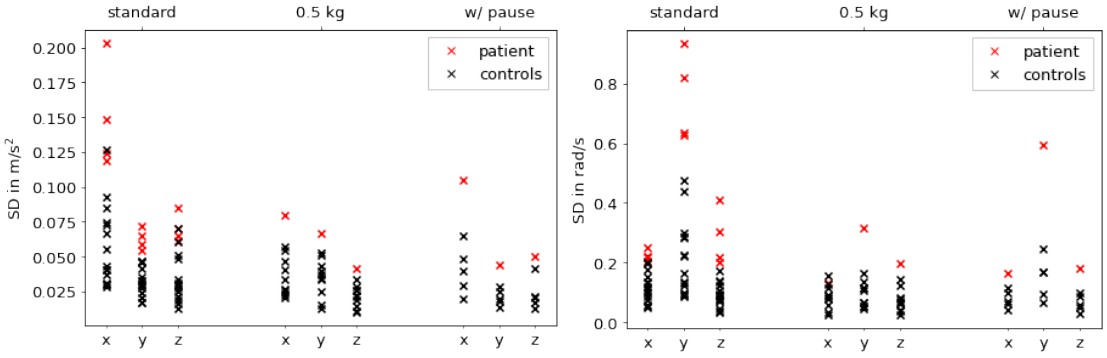

Figure 4: Standard deviation of the high frequency components for the acceleration and angular velocity of the pointing task for all three axes (x, y, z)

2.2.2 Static tasks

Standard deviation

Since for the flexion and extension tasks, the task was to hold the weight as still as possible, the standard deviation is a very simple measure for the instability of the patients hand. A high standard deviation indicates a less stable hand, because more movement was involved. We observed higher standard deviations for both, the flexion and extension tasks.

For the flexion tasks, fig. 5 shows that the standard deviation is higher for the patient than the controls for all axes in both the accelerometer signal and the gyroscope signal.

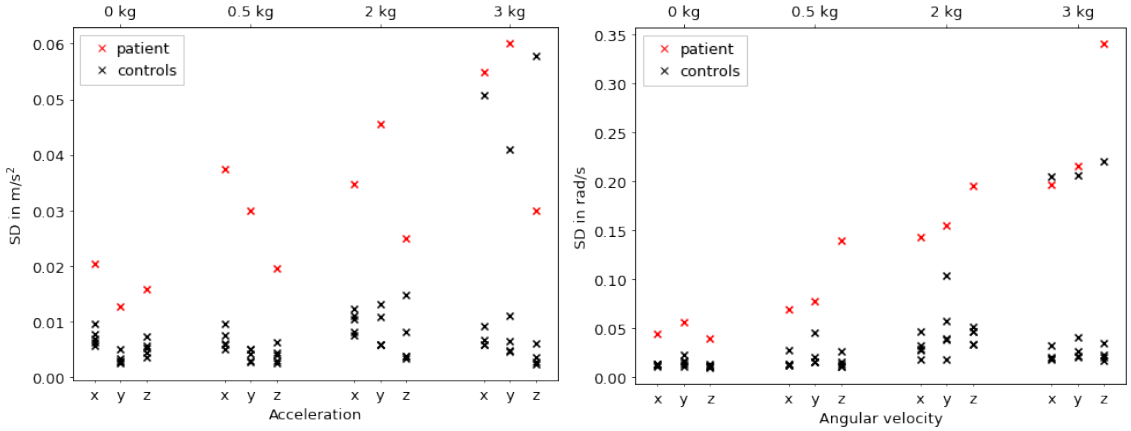

Figure 5: Standard deviations of the flexion tasks for all axis (x, y, z) and the two signals (accelerometer, gyroscope). The patient is marked in red and the control subjects in black.

Interestingly, the standard deviation is for the patient overall the highest along the x and y-axis which indicates forward and downward movement in the flexion task. While we expected a high downward movement because of the weight, we expected rather sideways movement than forward movements because forward movements would rather indicate shoulder movements than movements of the forearm. In addition, an increase of the standard deviation with a higher weight can be observed. This indicates that the patient was much weaker than the control subjects. The relative weakness of the patient was also noticeable during the experiment, although, it might not necessarily be related to the disease but could also be an individual feature. In future studies it might be advisable to only compare the weighted tasks within one patient and to document the strength of the arm over time. In contrast to the weighted tasks, the unweighted task can be compared to other healthy controls to track the instability. There, the patient had a higher standard deviation than the control subjects. So the hand of the patient was even without weight less stable than the controls' hands. Overall, the instability of the patient is very significant, however, MIRAS might not be the main or only reason for the weakness of the patient.

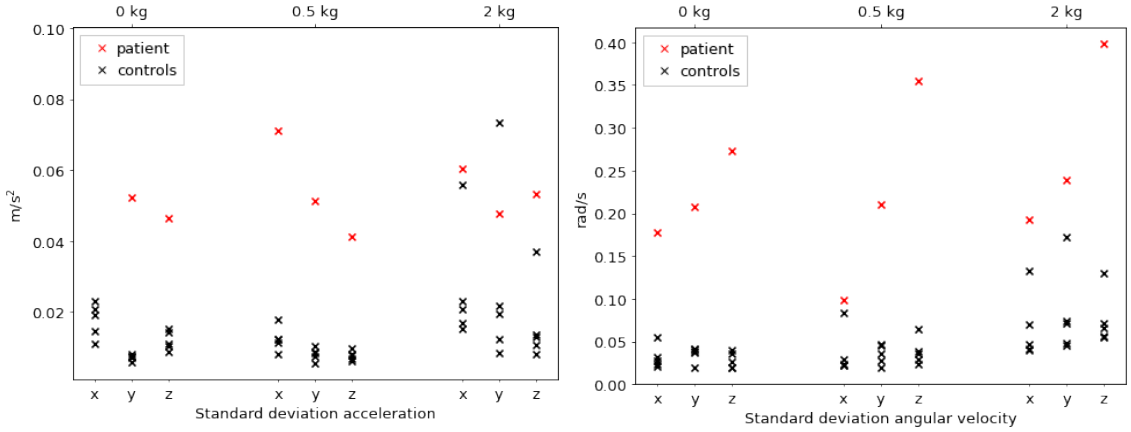

Figure 6: Standard deviations of the extension tasks for all axis (x, y, z) and the two signals (accelerometer, gyroscope). The patient is marked in red and the control subjects in black.

Similar to the flexion task, the patient has a relatively high standard deviation for the extension task. Overall the difference between the MIRAS patient and the controls is stronger here and also the absolute value of the standard deviation is greater than for the flexion task. These difficulties the patient had were also visible during the experiment itself. For the task with 2 kg the patient needed assistance from the instructors to hold the weight. This might also be the reason why no trend with increasing weight is visible here.

In general, for further investigations the analysis of the standard deviation of static tasks may only be meaningful if the different runs are comparable. It would be better to compare subjects with themselves and only perform tasks that can be executed by all subjects correctly and without help.

Mean-crossings and peak count

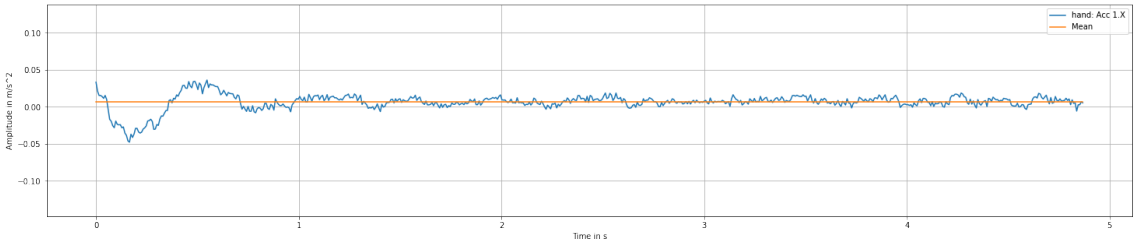

(a) Control subject

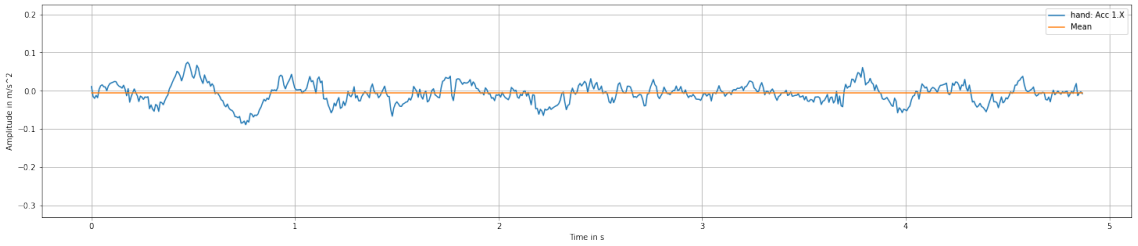

(b) Patient

Figure 7: x-axis acceleration signal of a control subject and the patient for the flexion task with 2 kg weight

Figure 7 shows that the signal for the control has values that are much closer to the mean than for the patient. The patient on the other hand has larger peaks indicating a more sudden movement. There are also fewer peaks visible for the patient than for the control. Further, it seems like the signal crosses the mean value less often for the patient because of the greater distance to the mean. To quantify these observations we will take a look at the mean-crossings and peak count as another two possible features for distinguishing patient and control.

As expected, the number of mean-crossings and the peak count is relatively low for the patient(see figure 8). While the mean-crossings stay more or less the same with increasing weight, the peak count for the acceleration shows a strong increase. This increase is also visible for the healthy subjects and especially visible on the x and z axis. In this task, a great acceleration along the x-axis corresponds to up and down movement and the z axis stands for movement from left to right, which are typical movements one performs when holding something heavy. Therefore, this plot indicates that the patient had a more unstable hand than the healthy subjects and was generally weaker than the patients.

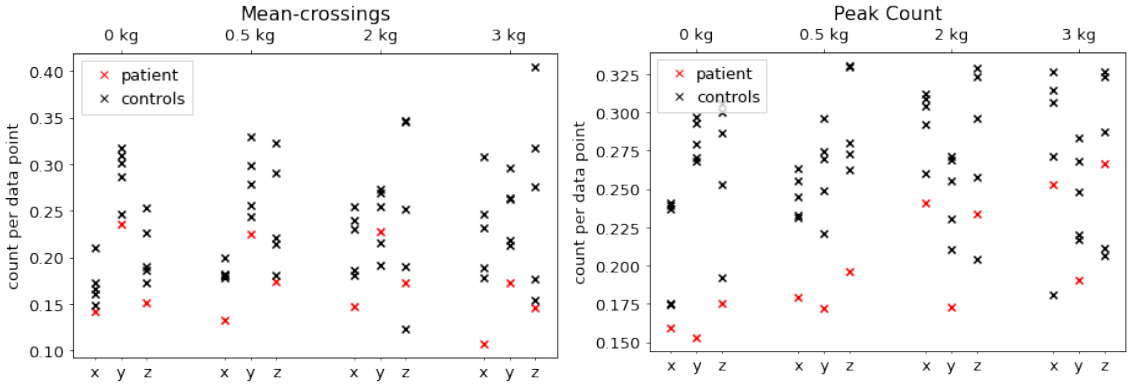

Figure 8: Mean-crossings and peak count for the acceleration signal of the flexion tasks for all axis (x, y, z).

However, this feature can only be observed for the flexion tasks and the acceleration data. The gyroscope signal and signals for the flexion task do not show this trend. In further studies with a larger amount of data it could be investigated whether the mean-crossings and the peak count are meaningful features overall.

Frequency Domain

Additionally, we computed the energies of the signal for frequency windows of 4 Hz. Here, the results were hard to interpret, because there were no outstanding differences between patient and control. The most obvious difference is, that the energy of the patient is overall higher, than the control. This however, correlates with the standard deviation and is therefore no new feature itself. For some flexion tasks, the patient had a relatively high energy for frequencies between 15 and 20 Hertz, whereas the most dominant energies of the control subject were at lower frequencies between 5 and 15 Hertz. Nevertheless, here the results were not very clear because there were also relatively high energies for the control subject between frequencies of 15 to 20 Hertz for some tasks. Overall, there might be no difference in frequencies which would imply that the movements of the patient were comparable with the ones of the controls but with a higher energy overall.

2.2.3 Feature Comparison

Table 3 provides an overview of the significance of individual features for different tasks.

It shows, that for different features different signals are more important than others. The angular velocity is for example good for analyzing the correlation of different repetitions whereas the accelerometer yields other useful features such as high frequency components of repetitive tasks or the number of mean crossings or the peak count for the flexion tasks. There are also features for which gyroscope data and accelerometer data seems to perform equally like the amplitude for repetitive tasks or standard deviation for static tasks. This shows that both, acceleration and angular velocity are important for the analysis. In future studies it would be advisable to include both, an accelerometer and a gyroscope sensor in the experimental setting.

	Period	Correlation		Amplitude		High frequencies	
		Acc	Gyro	Acc	Gyro	Acc	Gyro
Pointing standard	?	✗	✓✓	✓✓	✓✓	✓	✓
Pointing 0.5 kg	✓✓	✗	✓	✓✓	?	✓	✗
Pointing w/ pause	✗	✗	✓✓	✓✓	✓✓	✓✓	✓✓
Left/Right standard	✓✓	✗	✓	✗	✗	✗	?
Left/Right 0.5 g	✗	✓	✓	?	✗	✓✓	?
Pro/Supi	✓✓	✗	✗	✗	✗	?	✗

(a) Feature overview for repetition tasks

	Standard deviation		Mean-crossings		Peak count		Freq
	Acc	Gyro	Acc	Gyro	Acc	Gyro	
Flexion 0 kg	✓✓	✓✓	✓	✗	✓	✗	✗
Flexion 0.5 kg	✓✓	✓✓	✓	✗	✓✓	✗	✗
Flexion 2 kg	✓✓	✓✓	✗	✗	?	✗	✗
Flexion 3 kg	?	?	?	✗	✗	✗	✗
Extension 0 kg	✓✓	✓✓	✗	✗	✓	✗	✗
Extension 0.5 kg	✓✓	✓	?	✗	✓	✗	✗
Extension 2 kg	?	✓	?	✗	✗	✗	✗

(b) Feature overview for static tasks

Table 3:
✓: Feature distinguishes patient from control (very well ✓✓)
?: Feature might distinguish patient from control in further analyzes
✗: Feature does not distinguish patient from control

In addition, all the features analyzed for the repetitive task have a high significance, while for the static task mainly the standard deviation is an important feature. The other features analyzed for the static tasks do not show very clear results. Considering also the fact that the strength of the patient is not necessarily related to the disease, static tasks should only be compared within a subject to assess the progression of the disease. A feature that is not meaningful at all in our analysis is the energy of different frequency intervals. Nevertheless, specific frequency ranges might be of interest and might only not be visible in our analysis because of an insufficient amount of data.

2.3 Conclusion

This study showed clear differences of the IMU signal between the MIRAS patient and control subjects both in repetition and static tasks.

We identified a lower smoothness and regularity in the movement of the repetitive tasks, which could occur due to movement coordination difficulties caused by MIRAS. The patient also showed more sudden movements indicating a higher amount of involuntary movements, which possibly can be traced back to the disease as well. For the repetitive tasks, the maximal repetition amplitude, standard deviation of high frequency components, and correlation of repetitions have been identified as useful features for assessing the progression of MIRAS. Especially the repetitive tasks involving large and slow movements such as the Finger-to-nose test showed significant differences between patient and control subjects, while fast alternating hand movements could not distinguish patient and controls that well. Here, weighted tasks were not as meaningful as unweighted tasks and therefore might not be considered in future studies.

The static tasks showed a weakness of the arm of the patient but also for unweighted tasks a higher instability of the hand. Since strength could also be an individual feature, it might be

more meaningful to track weighted static tasks for a subject over time instead of comparing the strengths of multiple individual subjects.

Using the IMU signal is a more simple alternative to using an EMG signal. Some processing such as removing offsets and the gravity are still necessary. However, it cannot measure internal neurological processed but just the physical effects of the disease. Moreover, interpretation of single axes of the IMU sensor can be difficult and could be more comparable within one subject.

All in all, we conclude that IMU sensors can be suitable to detect MIRAS ataxia. However, since our dataset was relatively small, we suggest performing further studies including more age and weight matched control subjects. A larger dataset would also give the opportunity for a deeper Machine Learning analysis. Further, a glove with an integrated IMU sensor or a wrist-worn devise might be cheap and simple tools to perform the tasks at home. In a home-based environment, measurements could be done more regularly, for example twice a month, to also monitor the progression of MIRAS.

3 IMU arm measurement 2022

This section documents the measurements done in October 2022 using the Xsens MTw Awinda IMU sensors. The goal of this study was on the one hand to investigate the IMU sensors further and with a greater amount of data, but also to find the most meaningful positions of the sensors for these tests and to compare the results to standardized scales.

3.1 Measurements

3.1.1 Xsens MTw Awinda IMU sensors

For the measurements we used the Xsens MTw Awinda IMU sensors[1]. These are a human motion tracking system and consist of 3D linear accelerometers, 3D rate gyroscopes, 3D magnetometers and a barometer. Reasons why we switched from the Delsys Trigno Quattro Sensors to the Xsens MTw Awinda sensors include connection issues the Delsys sensors sometimes have, regular crashes of the Delsys EMG Logger App and the fact that we only have two Delsys Trigno Quattro sensors at the moment, while we have more than six Xsens MTw Awinda IMU sensors available.

The Xsens MTw Awinda IMU sensors are wirelessly connected to the Awinda base station, which is connected via USB to a Laptop. The base station is also used for charging the sensors. Measurements can be done with the Xsens MT Manager software. The sensors can be attached to the body using body straps [17].

The sampling frequency of the accelerometer and gyroscope of the Xsens MTw Awinda is 1000Hz. The sensors use on-board Strap-Down integration (SDI) [2] consisting of a low-pass filter at a bandwidth of 184 Hz, which is customized for movement analysis. Then, the processed signals are outputted at a user-selectable output frequency, which depends on the number of sensors that are connected to the Awinda base station. The magnetometer data is outputted at the same output rate as the accelerometer and gyroscope data [18]. The 3D acceleration is measured in m/s^2, 3D angular velocity (rate of turn) in rad/s and the 3D magnetic field in no SI unit, but it is normalized to the earth's field strength at the location the magnetic calibration was performed. All three signal are outputted in the sensor fixed coordinate system. [3] The free acceleration (acceleration without gravity) is measured as well and outputted in the local earth frame. [4] If one wants to use the free acceleration it would be good to rotate is into the sensor-fixed frame using the orientation data of the sensors. [5] However, we don't use the free acceleration in this analysis for two reasons. The first reason is that we want to compare the data to the data obtained in 2021 in the EMG analysis and there we also used raw acceleration in the sensor-fixed frame and removed the gravity with a Madgwick filter . The second reason is, that the free acceleration has a non-removable error at the beginning of the measurement. Further, the Xsens MTw Awinda software includes the Xsens Kalman filter. The orientation of the Sensor can be outputted in Euler representation, unit quaternions or as a rotation matrix.

Detailed instructions and information can be found in the Xsens MTw Awinda manual [17], the Xsens MTw Awinda whitepaper [18] or in the Xsens catalog[6].

3.1.2 Tasks

Because the Finger-to-nose test (Pointing task/FNT) (see fig. 9a) showed clear differences between patient and control, we included this tasks in the new measurements again. However, we removed the modifications from the task since they did not improve the results. In this test, besides the IMU data a rating on the SARA scale [4] is done by a clinician. The FNT is performed eight times in total with five alternating movements from nose to point and back like in the previous study.

[1] https://www.xsens.com/products/mtw-awinda
[2] https://base.xsens.com/s/article/Understanding-Strapdown-Integration?
[3] https://mtidocs.xsens.com/mti-system-overview$calibrated-inertial-and-magnetic-data-outputs
[4] https://mtidocs.xsens.com/mti-system-overview$free-acceleration
[5] https://base.xsens.com/s/article/Transforming-MTi-data-from-local-frame-L-to-sensor-frame-S?
[6] https://base.xsens.com/s/topiccatalog?language=en_US

(a) Finger-to-Nose Test (b) Box and Blocks Test (c) 9-Hole Peg Test

Figure 9: Performed tasks

Additionally, we included the Box and Block Test (BBT) (see fig. 9b), a standardized neurological test for measuring gross manual dexterity[7]. Here the subject has to transfer as many blocks as possible from one side of a box to the other in 60 seconds. The number of boxes transferred is measured. For the BBT the subject has a 15-second trial period before performing the task twice in total.

Further, we included the Nine-Hole Peg Test (9HPT) (see fig. 9c), another standardized neurological test to measure smaller finger dexterity[8]. In this test, the subject has to place nine pegs as fast as possible into holes of a board and then remove them. Here, the time period how long it takes the patient to perform the task is measured. In this task the patient has a trial before the actual measured task as well. The task is then performed twice.

3.1.3 Participants

11 control subjects took part in the study. Due to an unknown issue the sensors stopped recording the measurement of participant F after the Box and Blocks test. Therefore, the 9-Hole Peg Test and the second pointing task was repeated on another day. One participant (G) was left-handed. However, he said that he also performs many daily tasks with his right hand. Therefore, we did the measurements for both sides (the GR data is the data of his right hand and the GL data is the data of his left hand). His performance was very similar with both hands. In the following analysis only the right hand is included in the results. However, there is still the possibility to use the left-hand data and mirror it accordingly. An overview of all participants shows table 4.

ID	Date	Gender	Handedness	Age [years]	Weight [kg]	Height [cm]
A	05.10.2022	F	R	30	59	159
B	05.10.2022	F	R	27	59	165
C	05.10.2022	F	R	28	53	165
D	05.10.2022	M	R	30	130	183
E	06.10.2022	M	R	29	85	189
F	06.10.2022/10.10.2022	M	R	44	77	178
G	06.10.2022	M	L	30	63	170
H	07.10.2022	F	R	21	52	169
I	10.10.2022	M	R	31	65	172
J	10.10.2022	M	R	30	81	175
K	13.10.2022	F	R	32	43	155

Table 4: Overview Participants

In the analysis the data of these control subjects is compared to the data from 2021. Therefore, another five control subjects and the data of the patient are considered as well.

[7] https://www.physio-pedia.com/Box_and_Block_Test
[8] https://www.physio-pedia.com/Nine-Hole_Peg_Test

3.1.4 Study Setup

To obtain the complete arm movement of the subjects the measurements were done with four Xsens Awinda IMU sensors. The sensors were connected to the Awinda base station and the signal is recorded with the Xsens MT Manager. We measured the acceleration, angular velocity (rate of turn), magnetic field, free acceleration and orientation of the sensor over time. Since the output rates don't affect the accuracy of the output therefore, we use an output rate of 100 Hz for all signals.

Before the measurements, a calibration of the sensors is necessary to obtain the correct orientation of the sensors in relation to the body segments. Therefore, a heading reset is performed while the sensors are aligned as shown in figure 10a. [9]

Then, they were placed on the back of the hand using a glove and on the wrist (which is the same sensor position as in the previous study), the upper arm and the shoulder blade using straps, according to recommendations of the MTw Awinda manual [17] and Höglund et al [19]. All sensors on the arm and hand are oriented with the x-axis pointing along the distal axis of the arm. The sensor on the back is oriented so that the x-axis points down to earth along the gravity axis. For calibrating the sensors, the T-pose is measured. The orientation of all sensor in relation to the body and earth coordinate system is shown in figure 10b.

If one wants to use the orientation data of the sensors, in further measurements the calibration and performed tasks have to have the same orientation relative to the heading reset. This relation of the sensors to the earth-fixed coordinate system during the heading reset and the calibration is shown in fig. 10a and fig. 10b too. So the x-axis (blue) of the sensor points along the same axis as the arm of the subject. For all three tasks (FNT, BBT, 9HPT) the subject did not change its orientation compared to the calibration, so the line of sight of the subject always went along the light blue axis of the earth fixed orientation frame.

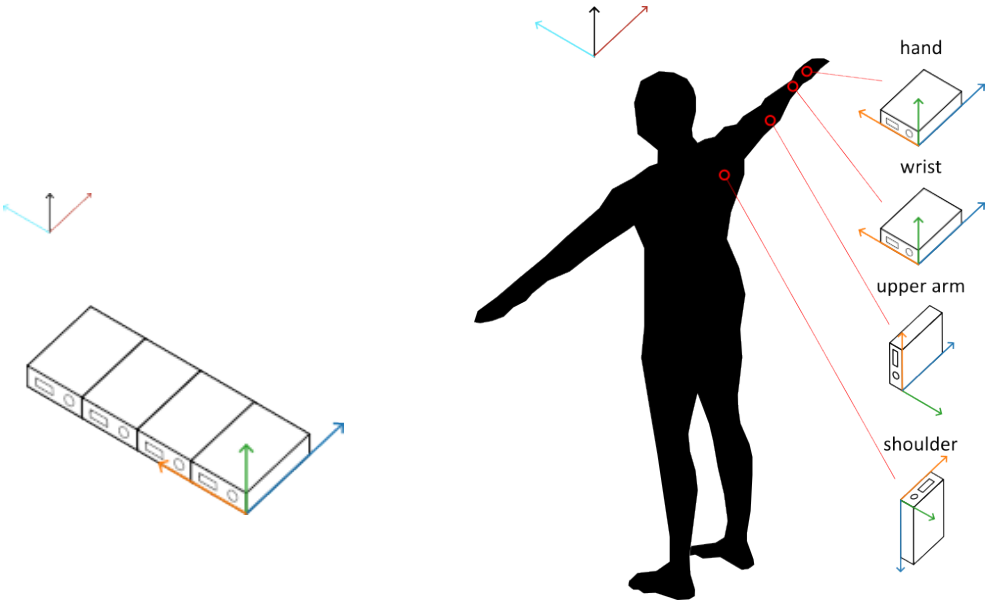

(a) Heading reset

(b) Calibration

Figure 10: Ideal orientation of the sensors and their sensor fixed coordinate system x(blue), y(orange) and z(green) in relation to an earth-fixed coordinate system

First, four sets of five repetitions each of the pointing task were performed. Then the subject could practice the BBT for 15 seconds and then had two recorded trials for it. After that the subject had a practice trial for the 9HPT and then performed it twice with recording. In the end, the pointing task was repeated with again four sets of five repetitions each.

[9] https://base.xsens.com/s/article/Changing-or-Resetting-the-MTi-reference-co-ordinate-systems-1605869706643?

A detailed description of the Study Setup can be found in *Study Protocol MIRAS IMU measurements.docx*

3.2 Data analysis

3.2.1 Data preprocessing

For comparison reasons, the preprocessing of the data was the same as for the IMU data from 2021.

The data was cut at the beginning and the end of the repetition and the gravity was removed with a Madgwick filter [16] like in the previous analysis. The data was further low-pass filtered with a cutoff frequency of 20 Hertz. The cutting is done manually in the columns *Start time* and *End time* of the *overview.xlsx* file. Another important thing to notice is that the x and y-axis of the Delsys and Xsens sensors are switched, which has to be considered when comparing the data.

3.2.2 Feature extraction

For the pointing task, the same features as in the previous analysis were extracted, namely the repetition period, the repetition correlation, the repetition amplitude and the standard deviation of the high frequency components (cutoff frequency 5 Hertz). With these features we can extend the control group and verify the usefulness of the features.

Since there was too little time, and we don't have data of the patient for the BBT and 9HPT yet, I did not extract any features for those two tasks. However, I have some ideas which features might be useful.

For the BBT I have the following ideas:

- Blocks count: The blocks count is a natural way of assessing the BBT. It could be used as a reference measure and also could be a good indicator of the progression of the disease (decreasing count). The blocks count is noted in the *overview.xlsx* file of each subject.
- Features of single repetitions: I already tried splitting the signal into the single repetitions using the same script as for the pointing task. However, this did not work because the repetitions seem less regular. Maybe the single repetition can still be extracted with an improved script. Then features like the amplitude, correlation, etc. could be investigated.
- Standard deviation, frequency domain, etc.

For the 9HPT I have the following ideas:

- Total time: Like the blocks count for the BBT, the total time is the standard way of assessing the 9HPT and is noted in the *overview.xlsx* File of each subject.
- Input/removal time: Only the time it takes the subject to put the pegs into the board or remove them. The ratio of the input/removal time might also be an interesting feature. The time point when the subject removes the pegs can be easily observed (see fig. 11). I have already defined some of these time points in the *Middle time* column of the *overview.xlsx* file and split the signal according to this.
- Features of single repetitions: I did not try this yet, but because this test has fewer repetitions than the BBT, it might be easier splitting the repetitions here. Then features like the amplitude, correlation, etc. could be investigated.
- Standard deviation, frequency domain, etc.

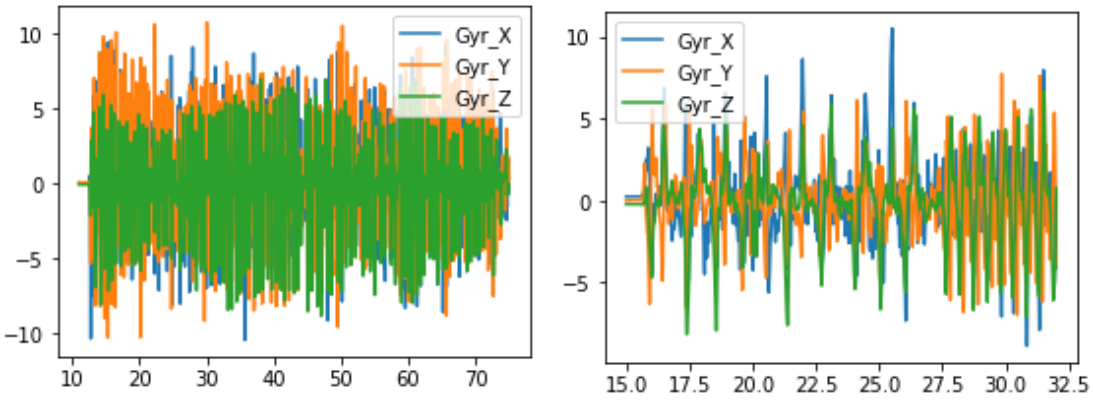

Figure 11: Example signal of the BBT (left) and 9HPT (right)

3.3 Results and Discussion

Here, only the discussion of the results of the comparison between the old and new control data for the standard pointing task is done. Additionally, to the comparison with the patient, a comparison of each subject to both control groups was done to investigate individual outliers.

3.3.1 Repetition period

In the previous analysis the patient tended to have a relatively high repetition period compared to all subjects. However, this analysis showed that the repetition period is highly individual and that the repetition period of the patient is not significantly different to the control group (see fig. 12).

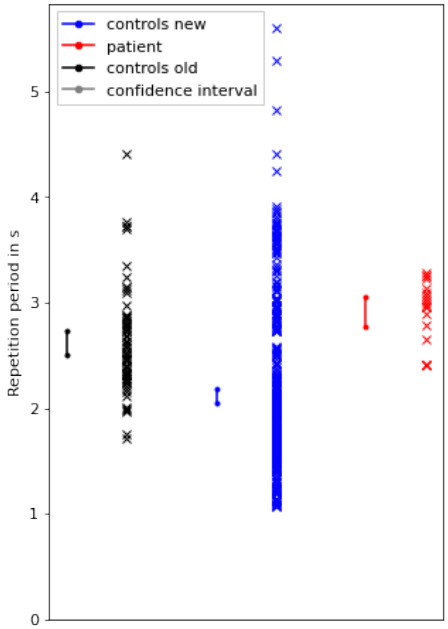

Figure 12: Comparison repetition period patient, old control group and new control group

The full comparison of all subjects to the control group shows that subject D performed the task relatively slow whereas subject B, E and J performed it relatively fast (see fig. 16). This might be because the subject were asked to perform the pointing at their own speed and therefore there are people with a relatively small repetition period but also people with a high repetition

period. Further, for some subjects the repetition periods of the tasks performed after the speed tests were noticeable faster than for the tasks performed before the speed tests.

All in all, we conclude that the repetition period is no meaningful feature and that it should not be considered in further analyzes.

3.3.2 Repetition Correlation

The repetition correlation of the gyroscope data was a meaningful feature for the control group of 2021 with the patient having a relatively low correlation (see fig. 13). The correlation of the new control group is about the same as the correlation of the old control group and therefore the new control group verifies the repetition correlation as a meaningful feature.

The full comparison of all subject shows that some subjects (D and SR) have a lower correlation than the control groups (see fig. 17). Especially subject SR has a similarly low correlation for the acceleration signal. For the gyroscope signal, no other subject has such a low correlation as the patient.

Therefore, especially the correlation of the gyroscope signal is a meaningful feature. The difference between patient and controls is here very high and no other subject shows this difference. The correlation of the acceleration is on the lower end of the scale compared to the other subjects. A reason why there is no such big difference as in the gyroscope signal might be that the acceleration correlation is quite low in general for all subjects.

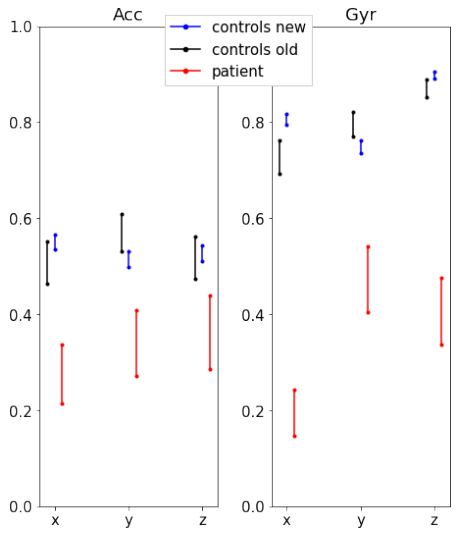

Figure 13: Comparison repetition correlation patient, old control group and new control group

3.3.3 Repetition Amplitude

The amplitudes of the new control group are similar to the amplitudes of the old control group for the acceleration data. The patient still stands out with large amplitudes of the x-axis of the acceleration data and the y-axis of the gyroscope data (see fig. 14). However, the other axes are less meaningful, even though there is a difference visible for the acceleration amplitude.

In the full comparison, the weight-matched control subject also stands out along those two axes 18. However, the absolute value of the amplitude intervals is lower that for the patient, which indicates that the patient still stands out from the controls. The other subjects don't stand out with a high amplitude.

To conclude, this shows that the repetition amplitude is still a meaningful feature, however, only two axes seem to be very relevant.

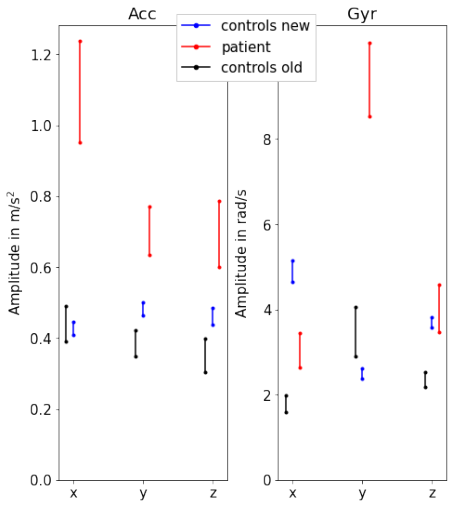

Figure 14: Comparison repetition amplitude patient, old control group and new control group

3.3.4 High frequency components

The MIRAS patient still stands out in terms of high frequency components along the x-axis of the acceleration data and the y-axis of the gyroscope signal (see fig. 15). However, the other axes for which the patient also was on the higher end of the range aren't meaningful anymore.

In the full comparison of the high frequency components no other subject stands out like the patient. However, the matched control VR also has a relatively high amount of high frequency components and is on the upper end of the scale, still the absolute value is lower than the values for the MIRAS patient.

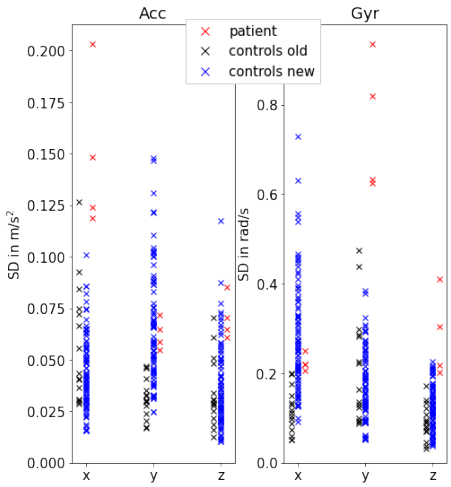

Figure 15: Comparison high frequency components patient, old control group and new control group

The different IMU sensor might also influence the result of this feature because the Xsens Awinda IMU sensors preprocess already some data during collection. Further, we used another sampling frequency, which might affect the result.

Still, high frequency components seem to be relevant to the analysis and should be considered in further studies.

3.4 Conclusion and further ideas

All in all, the results show, that three of the four features of the pointing task seem to be stable to new control data. The repetition period is not stable to the new control group and therefore should not be considered in further analyzes. The results also show that no other subject stands out as much from the control group as the patient.

The next steps include more measurements for MIRAS patients to also extend the patient data set and to check if the features still hold. Then, an analysis of the other sensor positions can also be done to identify the most meaningful sensor positions and in the end to design an easily wearable sleeve/glove for IMU sensors. Because of the higher number of control subjects, higher number of repetitions for each task and the additional sensors there is also more data available, so that machine learning methods could be applied too.

The Box and Blocks test as well as the 9-Hole Peg Test could be analyzed also. The new Xsens Awinda sensors also give the opportunity to get meaningful data from the orientation of the sensors, for example to compute the angles between the single body segments. Further, they also compute the free acceleration which could be used instead of the Madgwick filter in further analyzes. However, the free acceleration has an onset at the beginning of the heading reset, of which the reasons should be investigated first before using this signal.

References

[1] A. H. Hakonen, S. Heiskanen, V. Juvonen, I. Lappalainen, P. T. Luoma, M. Rantamäki, G. V. Goethem, A. Löfgren, P. Hackman, A. Paetau, S. Kaakkola, K. Majamaa, T. Varilo, B. Udd, H. Kääriäinen, L. A. Bindoff, and A. Suomalainen, "Mitochondrial DNA polymerase W748S mutation: a common cause of autosomal recessive ataxia with ancient European origin," *American journal of human genetics*, vol. 77, no. 3, pp. 430–441, 2005.

[2] M. Mancuso, D. Orsucci, and G. Siciliano, "Mitochondrial Ataxias," in *Ataxia: Causes, Symptoms and Treatment*, 1st ed., S. H. Hong, Ed. Nova Science Publishers, Inc., 2012, ch. 4, pp. 77–101.

[3] B. H. Cohen, P. F. Chinnery, and W. C. Copeland, "POLG-related disorders," *GeneReviews®*, 2018. [Online]. Available: https://www.ncbi.nlm.nih.gov/books/NBK26471/

[4] T. Schmitz-Hübsch, S. T. D. Montcel, L. Baliko, J. Berciano, S. Boesch, C. Depondt, P. Giunti, C. Globas, J. Infante, J. S. Kang, B. Kremer, C. Mariotti, B. Melegh, M. Pandolfo, M. Rakowicz, P. Ribai, R. Rola, L. Schöls, S. Szymanski, B. P. V. D. Warrenburg, A. Dürr, T. Klockgether, and R. Fancellu, "Scale for the assessment and rating of ataxia: development of a new clinical scale," *Neurology*, vol. 66, no. 11, pp. 1717–1720, 2006.

[5] T. O. Mera, D. A. Heldman, A. J. Espay, M. Payne, and J. P. Giuffrida, "Feasibility of home-based automated Parkinson's disease motor assessment," *Journal of Neuroscience Methods*, vol. 203, no. 1, pp. 152–156, 2012.

[6] A. Mueller, E. Paterson, A. McIntosh, J. Praestgaard, M. Bylo, H. Hoefling, M. Wells, D. R. Lynch, C. Rummey, M. L. Krishnan, M. Schultz, and C. J. Malanga, "Digital endpoints for self-administered home-based functional assessment in pediatric Friedreich's ataxia," *Annals of Clinical and Translational Neurology*, vol. 8, no. 9, pp. 1845–1856, 2021.

[7] M. Grobe-Einsler, A. T. Amin, J. Faber, T. Schaprian, H. Jacobi, T. Schmitz-Hübsch, A. Diallo, S. T. du Montcel, and T. Klockgether, "Development of SARA^{home} , a New Video-Based Tool for the Assessment of Ataxia at Home," *Movement disorders : official journal of the Movement Disorder Society*, vol. 36, no. 5, pp. 1242–1246, 2021.

[8] T. Dorszewski, W. Jiang, and S. Sigg, "Detection of an Ataxia-type disease from EMG and IMU sensors," in *2022 IEEE International Conference on Pervasive Computing and Communications Workshops and other Affiliated Events (PerCom Workshops)*, 2022, pp. 712–717.

[9] K. Terayama, R. Sakakibara, and A. Ogawa, "Wearable gait sensors to measure ataxia due to spinocerebellar degeneration," *Neurology and Clinical Neuroscience*, vol. 6, no. 1, pp. 9–12, 2018.

[10] A. Matsushima, K. Yoshida, H. Genno, A. Murata, S. Matsuzawa, K. Nakamura, A. Nakamura, and S. Ikeda, "Clinical assessment of standing and gait in ataxic patients using a triaxial accelerometer," *Cerebellum & ataxias*, vol. 2, no. 1, p. 9, 2015.

[11] N. Nguyen, D. Phan, P. N. Pathirana, M. Horne, L. Power, and D. Szmulewicz, "Quantification of Axial Abnormality Due to Cerebellar Ataxia with Inertial Measurements," *Sensors (Basel, Switzerland)*, vol. 18, no. 9, 2018.

[12] O. Martinez-Manzanera, T. F. Lawerman, H. J. Blok, R. J. Lunsing, R. Brandsma, D. A. Sival, and N. M. Maurits, "Instrumented finger-to-nose test classification in children with ataxia or developmental coordination disorder and controls," *Clinical biomechanics (Bristol, Avon)*, vol. 60, pp. 51–59, 2018.

[13] B. Oubre, J. F. Daneault, K. Whritenour, N. C. Khan, C. D. Stephen, J. D. Schmahmann, S. I. Lee, and A. S. Gupta, "Decomposition of Reaching Movements Enables Detection and Measurement of Ataxia," *Cerebellum (London, England)*, vol. 20, no. 6, pp. 811–822, 2021.

[14] R. Krishna, P. N. Pathirana, M. Horne, L. Power, and D. J. Szmulewicz, "Quantitative assessment of cerebellar ataxia, through automated limb functional tests," *Journal of Neuro-Engineering and Rehabilitation*, vol. 16, no. 1, 2019.

[15] N. C. Khan, V. Pandey, K. Z. Gajos, and A. S. Gupta, "Free-Living Motor Activity Monitoring in Ataxia-Telangiectasia," *Cerebellum (London, England)*, vol. 21, no. 3, pp. 368–379, 2022.

[16] S. O. H. Madgwick, A. J. L. Harrison, and R. Vaidyanathan, "Estimation of IMU and MARG orientation using a gradient descent algorithm," in *2011 IEEE International Conference on Rehabilitation Robotics*, 2011, pp. 1–7.

[17] *MTw Awinda User Manual*, ©Xsens Technologies B.V., 2018, Document MW0502P.L. [Online]. Available: https://www.xsens.com/hubfs/Downloads/Manuals/MTw_Awinda_User_Manual.pdf

[18] M. Paulich, M. Schepers, N. Rudigkeit, and G. Bellusc, "Xsens mtw awinda: Miniature wireless inertial-magnetic motion tracker for highly accurate 3d kinematic applications," ©Xsens Technologies B.V., Tech. Rep., 2018. [Online]. Available: https://www.xsens.com/hubfs/3446270/Downloads/Manuals/MTwAwinda_WhitePaper.pdf

[19] G. Höglund, H. Grip, and F. Öhberg, "The importance of inertial measurement unit placement in assessing upper limb motion," *Medical Engineering & Physics*, vol. 92, pp. 1–9, 2021.

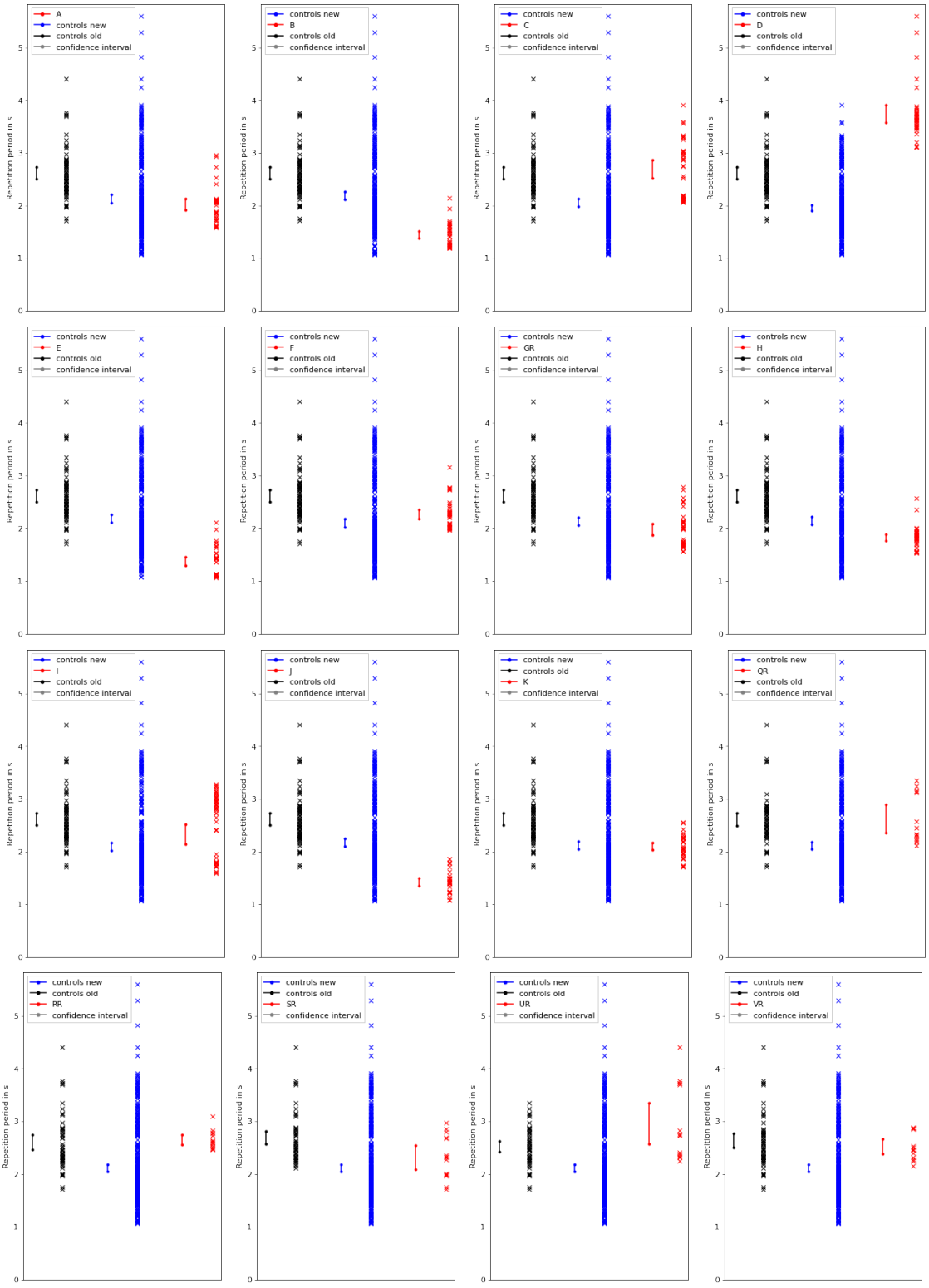

Figure 16: Individual comparison of the repetition period of each subject with the remaining control subjects

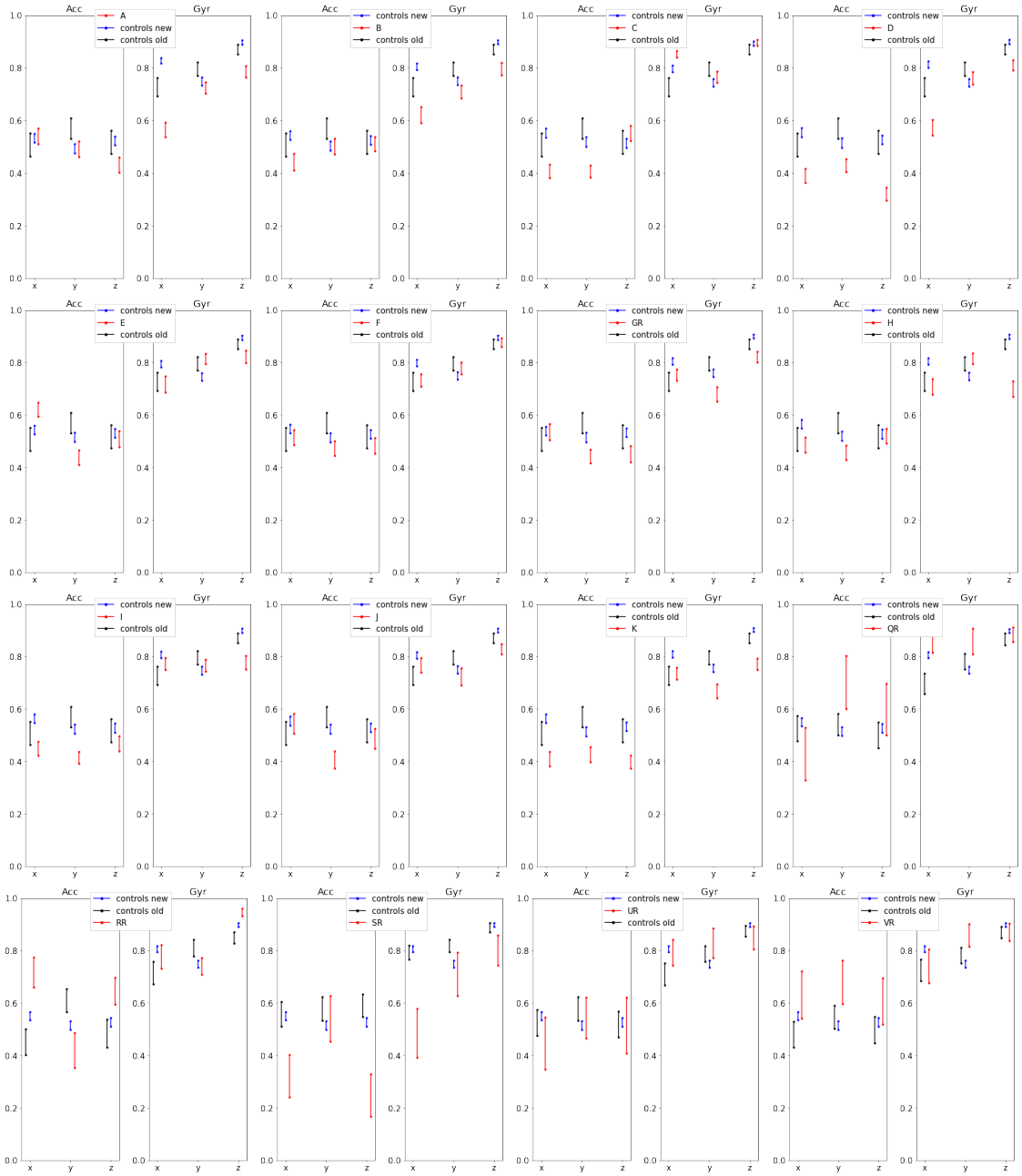

Figure 17: Individual comparison of the correlation of each subject with the remaining control subjects

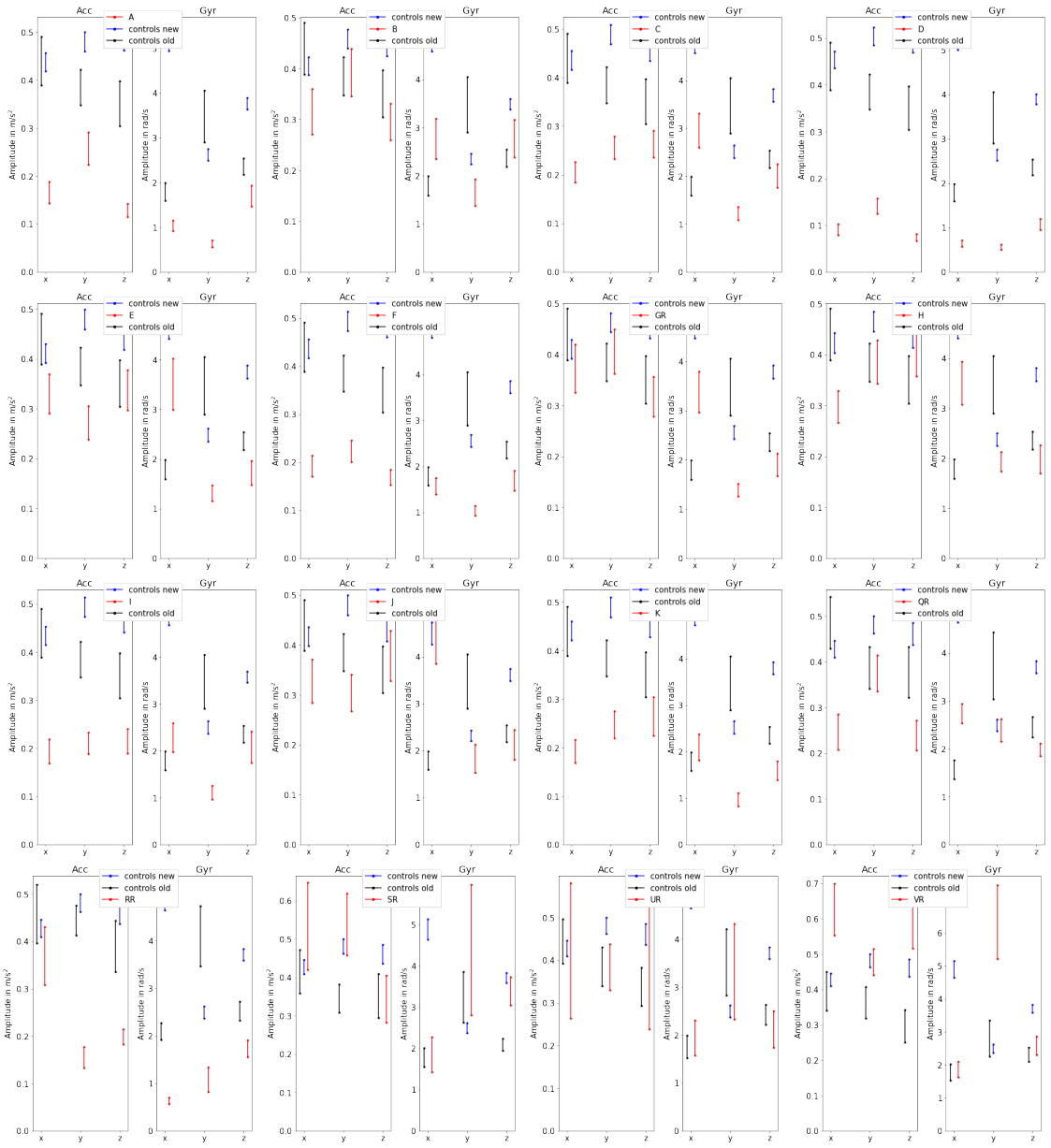

Figure 18: Individual comparison of the amplitude of each subject with the remaining control subjects

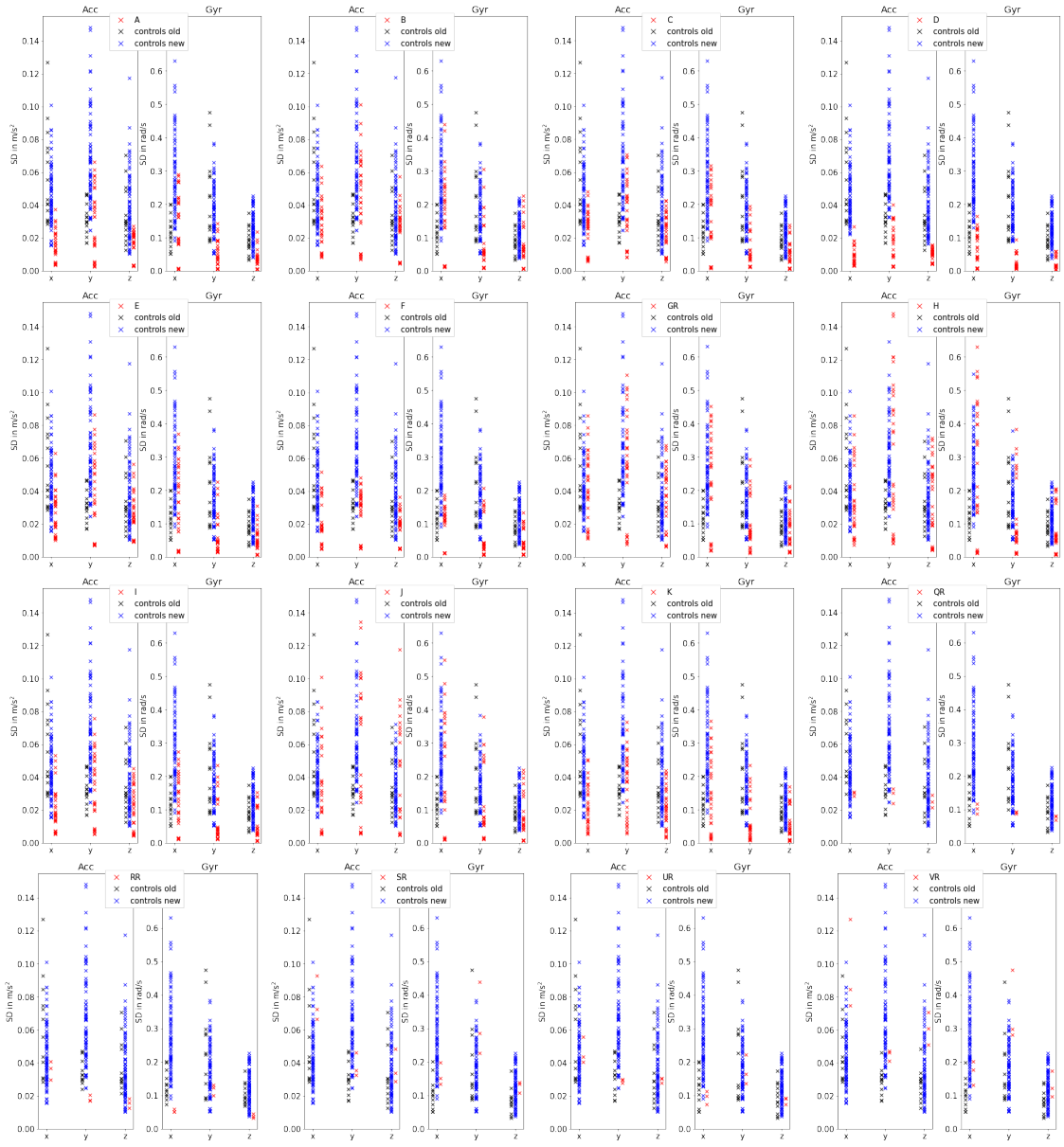

Figure 19: Individual comparison of the standard deviation high frequency components of each subject with the remaining control subjects